Journal of Applied Polymer Science

Thermomechanical and Shape Memory Properties of Thermosetting Shape Memory Polymer Under Compressive Loadings

J. T. Fulcher,[1] H. E. Karaca,[1] G. P. Tandon,[2,3] Y. C. Lu[1]

[1]Department of Mechanical Engineering, University of Kentucky, Lexington, KY

[2]Air Force Research Laboratory, Materials and Manufacturing Directorate, AFRL/RXCC, Wright-Patterson AFB, OH

[3]University of Dayton Research Ins., 300 College Park, Dayton, OH

Correspondence to: Y. C. Lu (E-mail: chlu@engr.uky.edu)

ABSTRACT: Shape memory polymers (SMPs) are an emerging class of active polymers that may be used for a range of reconfigurable structures. In this study, the thermomechanical and shape memory behavior of a thermosetting SMP was investigated using large-scale compressive tests and small-scale indentation tests. Results show that the SMP exhibits different deformation modes and mechanical properties in compression than in tension. In glassy state, the SMP displays significant plastic deformation and has a much higher modulus and yield strength in comparison to those obtained in tension. In rubbery state, the SMP behaves like a hyperelastic material and again has a much higher modulus than that obtained in tension. The SMPs were further conditioned separately in simulated service environments relevant to Air Force missions, namely, (1) exposure to UV radiation, (2) immersion in jet-oil, and (3) immersion in water. The thermomechanical and shape recovery properties of the original and conditioned SMPs were examined under compression. Results show that all the conditioned SMPs exhibit a decrease in T_g as compared to the original SMP. Environmental conditionings generally result in higher moduli and yield strength of the SMPs in the glassy state but lower modulus in the rubbery state. In particular, the UV exposure and water immersion, also weaken the shape recovery abilities of the SMPs.
 J. Appl. Polym. Sci. 129: 1096–1103, 2013

KEYWORDS: properties and characterization; mechanical properties; stimuli-sensitive polymers

Received 7 September 2012; accepted 30 October 2012; published online 23 November 2012
DOI: 10.1002/app.38791

INTRODUCTION

Shape memory polymers (SMPs) are active materials that can be used for various applications ranging from large structures such as aircraft wings to small devices such as micro-actuators.[1–7] SMPs have the ability to change shape in a predefined way from a temporary shape to a permanent shape when triggered through an external stimulus. The most commonly used stimulus for activating SMPs is thermal, which utilizes the temperature dependence of polymers as sketched in Figure 1. The typical steps used to thermally activate the SMPs have been described in details by Lendlein and Kelch,[1] Liu, et al.,[3] Xie,[4] Leng, et al.,[5] Gall,[8] and Tobushi, et al.[9] First, the SMP is activated at the deformation temperature, T_d, which should be above the material's glass transition temperature, T_g. At this stage, the SMP is in "rubbery" state and thus capable of undergoing large elastic deformation. Secondly, the constrained SMP is cooled to the storage temperature, T_s, which is below T_g. At this stage, the SMP is in "glassy" state and can withhold large forces. Finally, the SMP is heated up again to a recovery temperature, T_r, to allow the shape to recover freely. The recovery temperature may be a range of temperatures at which the SMP recovers its initial permanent shape during heating.

Different methods have been used to classify the SMPs.[1–5] In general, there are two types of SMPs: thermoplastic and thermoset. Thermoplastic SMPs have physical cross-links (intermolecular interactions) and thus can potentially melt at elevated temperatures. On the other hand, thermoset SMPs are chemically cross-linked (covalent bonded) and thus stable at elevated temperatures. In comparison, thermoset SMPs often exhibit much higher stiffness and dimensional stability, and have better environmental durability. Therefore, thermosetting SMPs have received much of the attentions among the researchers. The thermomechancial behaviors of several thermoset SMPs have been reported.[10–14] However, the studies have been mostly conducted in tension mode. It is known that the mechanical behaviors of thermoset polymers (in both glassy and rubbery states) depend strongly upon the deformation modes. Under tensile force, thermoset polymers often exhibit infinitesimal elastic

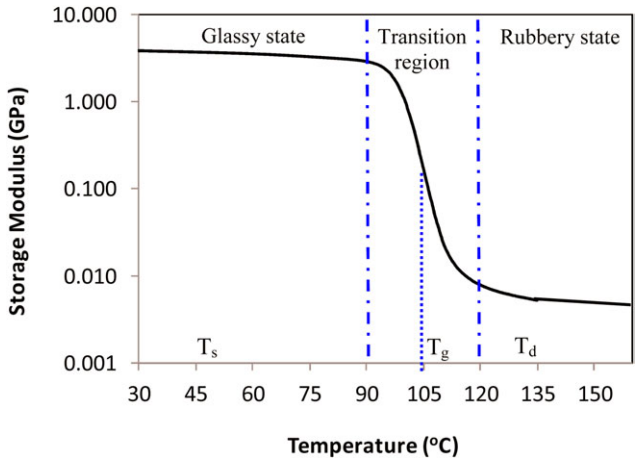

Figure 1. Temperature dependent properties of the thermosetting SMP (Veriflex-E). The storage moduli are measured from dynamic mechanical analysis (DMA) in torsional mode. [Color figure can be viewed in the online issue, which is available at wileyonlinelibrary.com.]

deformation below the transition temperature. They exhibit superelasticity above the transition temperature, but the resultant recovery forces are often low. The main purpose of this work was to comprehensively examine the thermomechanical behavior of original and environmentally conditioned thermoset SMPs under compressive modes. Large-scale compression tests along with small-scale indentation tests (localized compression) were conducted on a commercial, thermoset SMP, and the thermomechanical and shape recovery properties of the material were examined.

EXPERIMENTAL

Materials and Sample Preparations

The material studied was Veriflex-E, a two-part, fully formable thermoset SMP resin system developed by Cornerstone Research Group, Inc. (CRG).[16] Compared to other thermoset SMPs, the Veriflex-E has a relatively higher glass transition temperature (or transformation temperature), T_g –105°C,[15] which makes it suitable for aerospace structural applications. The uncured resin also has a low viscosity (0.2948 Pa.s at 25°C and 0.0531 Pa.s at 50°C), which makes it easy for processing and composite fabrication. Two types of samples were fabricated by the manufacturer (Cornerstone Research Group, Inc.) using the standard cure cycle.[16] For the first set, the SMP was compression molded into standard button-shaped specimens with a nominal diameter of 25.4 mm and a nominal thickness of 12.7 mm. These buttons were used for large-scale compression tests. For the second set, the SMP was molded into thin rectangular plaques measuring 300 mm by 300 mm with an average thickness of 3.2 mm. Smaller specimens, 10 mm × 5 mm, were subsequently cut from the larger plates for small-scale indentation tests. The surfaces of the small specimens were prepared by successive polishing, the final polishing compound being alumina with an average particle size of 0.3 μm.

To examine the mechanical behavior and shape memory properties of the SMPs in anticipated service environments, the SMP specimens (large buttons and small plaques) were conditioned relevant to Air Force missions. These included: (1) immersing SMPs in water at 49°C for four days, (2) immersing SMPs in lubricating oil at 49°C for 24 hours, and (3) exposing SMPs under ultraviolet (UV) radiation for 125 cycles (each cycle included 102 minutes of light only followed by 18 minutes of light and water spray). Further details on environmental conditioning can be found in reference.[12]

Large-Scale Compression Tests

The mechanical behavior of the SMP in the glassy state was first examined by performing large-scale compression test at room temperature (25°C). Tests were conducted in a servo-hydraulic MTS LandMark testing system through displacement control. A capacitive displacement sensor was used to measure the displacements. Since the material was very brittle at room temperature, the maximium compression was limited to 10% strain. The strain rate was varied from 0.00016 s^{-1} to 0.0016 s^{-1}. The mechanical behavior of the SMP in the rubbery state was examined using the same MTS LandMark testing system equipped with a custom built cooling-heating system. Omega CN8200 temperature controllers were used to control the temperature of the sample. The temperature was measured by a K-type thermocouples attached to the sample and compression grips. The samples were heated to 130°C using a 30 minute ramp time and then followed by a 30 minute dwell time to ensure thermal equilibrium. The specimens were pre-loaded with a 0.02 MPa stress to help ensure contact before initial capactive displacements were recorded. The specimens were compressed to a level of 30% strain from their original undeformed heights and then unloaded.

Small-Scale Indentation Tests

In addition to large-scale compression tests, small-scale indentation tests were also used to access the compressive properties of the SMPs. A localized compressive test, the instrumented indentation uses a small ball to press onto the specimen surfaces and the load-displacement response is recorded, from which the mechanical properties are extracted. Compared to large compressive tests, the indentation is more convenient in performing experiments over a wide range of loading rates and temperatures.

The indentation tests were performed on the MTS Nano Indenter XP (MTS NanoInstruments, Oak Ridge, TN). A spherical indenter (300 μm in tip diameter) was used. Compared to commonly used sharp indenters, the spherical indenter is more suitable for exploring elastic-plastic deformation of materials.[17–19] That is because the characteristic strain under a spherical indenter is directly proportional to the indentation depth. With the increase of indentation depth, the deformation in a material can change from purely elastic to elastic-plastic. The "held-at-the-peak" method was used for the indentation experiment, which is a technique used for testing polymer and soft materials.[20–23] In this method, the indenter was held at the maximum load for a length of time prior to unloading. This procedure allowed the material to relax and provoked the disappearance of the "bulge" on the initial unloading curve. The indentation tests were conducted at both room temperature and elevated

Applied Polymer SCIENCE

temperatures in order to access the mechanical properties of the SMPs as a function of temperature. Tests were performed at various loading rates and holding times. For each type of tests, a total of 10 measurements were replicated.

Shape Recovery Tests

The shape recovery abilities of the SMPs were examined under compressive loading. The large button-shaped specimens were tested. First, the samples were placed in the MTS LandMark machine and then heated to 130°C (30 minutes heating time and 30 minute dwell time). After the samples reached thermal equilibrium, they were deformed to a prescribed strain of 30%. Once the appopriate strain level was reached the displacment was held constant and the specimen was cooled to room temperature using a ramp time of 30 minutes. The height (thickness) of each specimen was measured and the sample photographed before beginning the recovery process. For recovery, a MTI KSL 1100X oven was used to heat each specimen to the prescribed recovery temperatures (60°C, 75°C, 105°C, 115°C, 130°C). A dwell time of 8 minutes was used for each stage of recovery and at each stage the sample heights were measured and specimens photographed to quantify the shape recovery properties of the SMPs.

RESULTS AND DISCUSSION

Mechanical Behavior of SMP in Glassy State

Compared to most thermoset SMPs, the present material Veriflex-E has a relatively higher glass transition temperature (–105°C). At room temperature, the material is in a glassy state and brittle. Figure 2 shows the stress–strain curve of the material obtained under compression (strain rate $\cong 3.4 \times 10^{-3}$ s^{-1}). The maximum compression on the sample was set to 10% of the original specimen height for safety consideration. For comparison, the stress–strain curve obtained in tension from previous study was also included.[12] There is a clear difference between the stress–strain responses obtained in tension and compression. Under tension, the material shows mostly elastic deformation and fractured at a small strain (approximately 5%). When tested in compression, the material exhibits an initial elastic response and then followed by almost perfectly plastic deformation. The modulus of elasticity calculated from the compressive stress–strain curve is 3.3 GPa, as compared to 1.6 GPa calculated from the tensile stress–strain curve. The yield strength (the maximum stress in stress–strain curve) obtained from the compressive stress–strain curve is 110.8 MPa, as compared to 77.8 MPa fracture strength obtained from the tensile stress–strain curve.

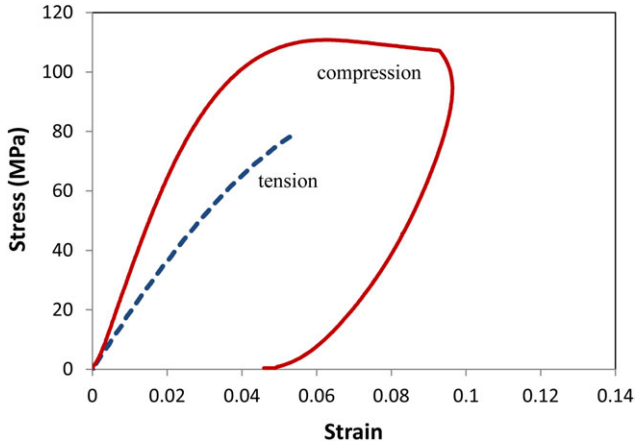

Figure 2. Comparison of the stress–strain curve of the thermosetting SMP in compression and tension (25°C). [Color figure can be viewed in the online issue, which is available at wileyonlinelibrary.com.]

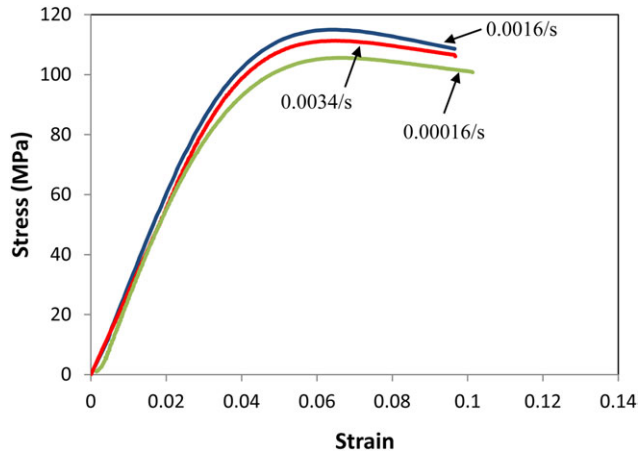

Figure 3. The compressive stress–strain curves of the thermosetting SMP under different strain rates (25°C). [Color figure can be viewed in the online issue, which is available at wileyonlinelibrary.com.]

The compressive tests were repeated at various strain rates, ranging from 0.00016 s^{-1} to 0.0016 s^{-1}, and the results are seen in Figure 3. In all cases, the SMP specimens exhibit large plastic deformation. As the strain rate increases, the modulus is seen to increase slightly from 3.15 GPa to 3.41 GPa, and the yield strength increases from 104 MPa to 115 MPa.

The mechanical properties of the SMP were further examined under localized compressive loading—the indentation test. Figure 4 depicts the load–depth curves of the present SMP indented

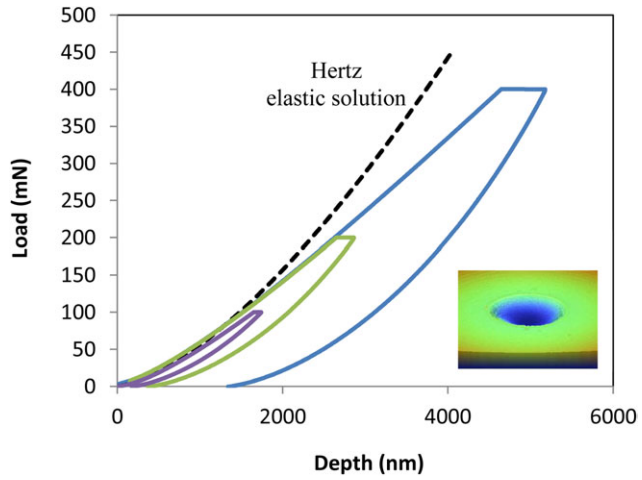

Figure 4. The load–depth curves of the thermosetting SMP under indentation loads (25°C). [Color figure can be viewed in the online issue, which is available at wileyonlinelibrary.com.]

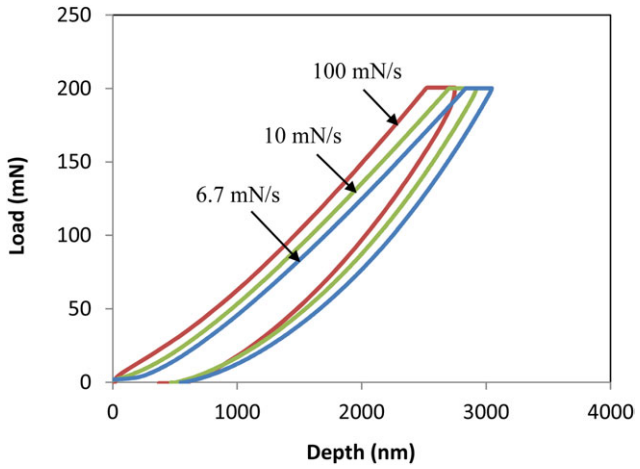

Figure 5. The indentation load–depth curves of the thermosetting SMP under different loading rates (25°C). [Color figure can be viewed in the online issue, which is available at wileyonlinelibrary.com.]

with the spherical ball (300 μm in diameter) at ambient temperature. The tests were conducted with progressively increasing loads up to a maximum of 400 mN. The loading time was 30 seconds and the indenter holding time 10 seconds. For comparison, the load-depth response calculated from Hertz's elastic solution was also included:[24] $F = \frac{2\sqrt{2}}{3}\left(\frac{E\sqrt{2R}}{1-\nu^2}\right)h^{3/2}$, where R is the radius of the spherical indenter, and E and are the modulus and Poisson ratio of the material, respectively. The Poisson's ratio value of 0.35 was used for the current SMP. It is seen that the initial loading-depth responses are in relatively good agreement with the Hertzian theory, indicating that the deformation is mostly elastic. As the load increases, the measured load–depth curves deviate from the purely elastic solution, indicating the transition from elastic to elastic-plastic deformation in SMPs.

The indentation tests were further conducted at different loading speeds. The maximum load was set at 200 mN and the time to load/unload was varied from 0.5 to 60 seconds, which resulted in a variation of loading rate from 3 mN s^{-1} to 400 mN s^{-1}. Representative load–depth curves obtained at different loading rates are depicted in Figure 5. It is seen that as the loading rate increases, the load–depth curve gets stiffer.

To compute the modulus from the indentation tests, the load–depth curves were analyzed, following the method developed earlier.[23–27] When an indenter is loaded to a depth (h_{max}) and then unloaded at a rate of $\dot{P}$, the indentation strain rate, $\dot{\varepsilon}_{in}$, may be approximated as

$$\dot{\varepsilon}_{\text{in}} = \frac{\dot{P}}{S \cdot h_{\max}} \tag{1}$$

where S is the elastic stiffness as determined from the slope of initial unloading curve, $S = (dP/dh)_{h=h_{max}}$.

The elastic contact depth (h_c) between the indenter and specimen is estimated

$$h_c = (h_{\max} - h_{\text{creep}}) - 0.75P_{\max}\left(\frac{1}{S} - \frac{\dot{h}_v}{\dot{P}}\right) \tag{2}$$

where h_{creep} is the change in the indentation depth during the holding time, P_{max} is the peak load, and $\dot{h}_v$ is the creep rate at the end of indenter holding segment.

The indenter-sample contact radius (a) is then calculated via the standard procedure

$$a = \sqrt{2h_cR - h_c^2} \tag{3}$$

The reduced modulus of the contact pair is calculated following the standard Oliver-Pharr procedures[25–26]

$$E_r = \frac{\sqrt{\pi}}{2 \cdot (1.034)}\frac{S}{\sqrt{\pi a^2}} \tag{4}$$

Finally, the elastic modulus E of the testing sample is

$$E = \frac{1-\nu^2}{\frac{1}{E_r} - \frac{1-\nu_i^2}{E_i}} \tag{5}$$

where E_i and ν_i are the elastic modulus and Poisson's ratio of the indenter (for diamond indenter: E_i = 1140 GPa and ν = 0.07).

The moduli of the SMP obtained at compressive loadings are plotted as a function of strain rate, as shown in Figure 6. Again, the large-scale compressive tests were mostly conducted at lower strain rates due to the safety consideration. Due to its non-destructive nature, the small-scale indentation tests were conducted over a broad range of loading rates and holding times. The use of indenter holding segment was to help obtain the corrected stiffness; different holding times do not change the material properties (modulus). The strain rates from indentation experiments are estimated using eq. (1). It is seen that the modulus increases gradually at lower strain rates and then raises dramatically at higher strain rates. Further, both large-scale compression and small-scale indentation tests result in similar

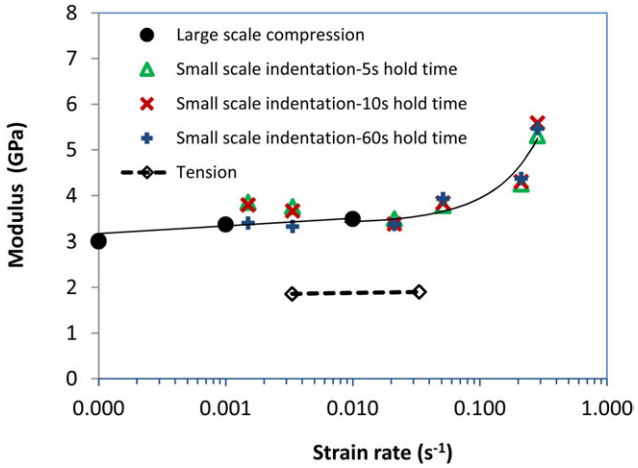

Figure 6. Strain rate dependence of the thermosetting SMP under compressive and tensile loading (25°C). [Color figure can be viewed in the online issue, which is available at wileyonlinelibrary.com.]

Applied Polymer SCIENCE

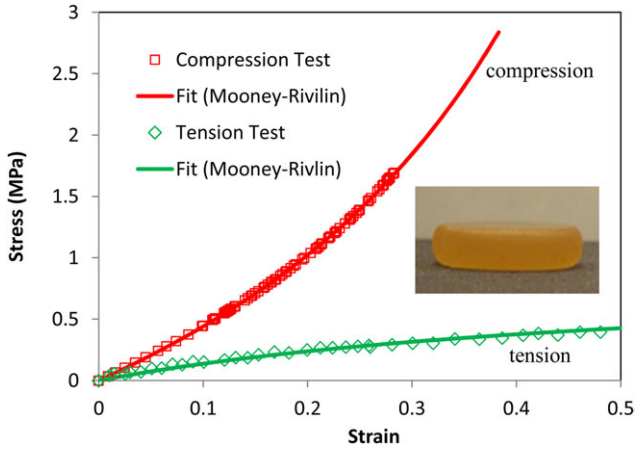

Figure 7. The stress–strain curve of the thermosetting SMP under compression and tension (130°C). [Color figure can be viewed in the online issue, which is available at wileyonlinelibrary.com.]

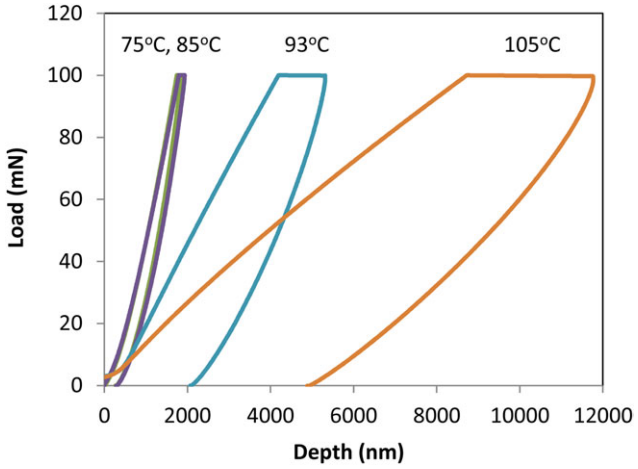

Figure 8. The indentation load–depth curves of the thermosetting SMP during the transition region. [Color figure can be viewed in the online issue, which is available at wileyonlinelibrary.com.]

values of compression modulus at the lower strain rate conditions. On the other hand, previously obtained results under tension[12] show lesser sensitivity to strain rates investigated.

Mechanical Behavior of SMP in Rubbery State

Figure 7 shows the stress–strain response of the SMP tested in compression at 130°C, which is above its glass transition region. At elevated temperatures, the SMP is hyperelastic and thus incompressible. When compressed, the button shaped specimen is seen to bulge out (the inserted picture in Figure 7), behaving as a typical rubber-like material. For safety concern, the maximum compressive strain was limited to 30%. For comparison, the stress–strain curve obtained earlier in tension is also included.[12] It is seen that the material is much stronger in compression than in tension in rubbery state. The stress–strain curves from the rubbery state can be closely fitted with classic hyperelastic model, i.e., the Mooney–Rivlin model[28]

$$\frac{\sigma}{(\lambda-\lambda^{-2})}=2C_{10}+\frac{1}{\lambda}2C_{01} \tag{6}$$

where λ is the stretch ($\lambda = 1+\varepsilon$), ε is the strain. C_{10} and C_{01} are coefficients from which the initial shear modulus is calculated [$G = 2(C_{10}+C_{01})$]. 29 The initial modulus of the SMP is calculated as 1.30 MPa under compression as compared to 0.54 MPa under tension, a 2.5 fold increase.

Mechanical Behavior of SMP in Transition State

To evaluate the mechanical properties of the SMP within the transition stage (90°C < T < 120°C), the indentation tests were performed on small size samples (10 mm × 5 mm × 3.2 mm). In this narrow transition region, the SMP changed its properties dramatically as temperature increased. Compared to larger macroscopic tests, the indentation test utilized much smaller specimens so that the temperature gradient within the samples was minimized. In the present test, the sample was placed on a microheater (3 cm in diameter), on which the SMP specimen was mounted. A separate thermocouple was attached to the specimen to monitor its true temperature. Figure 8 shows the load–depth curves of the material at several temperatures within the transition region. It is seen that the load–depth curves change greatly within this narrow temperature region. Following the same procedure [eqs. (1–5)], the moduli of the SMP within this region were calculated, as shown in Figure 9. It is seen that the present SMP exhibits a plateau modulus at both glassy and rubbery states. Under compression, the SMP has a large modulus variation from glassy to rubbery state: 0.05 GPa < E < 3.29 GPa, indicating that it has a wide range of tunable stiffness. The present SMP also has a "sharp" transition which is advantageous for the prompt "fixing" of the material at low temperatures and then the quick recovery at high temperatures.

Effect of Environmental Conditioning

Like conventional polymers, the SMPs can also undergo physical and chemical degradation when exposed to service environments. Thus, it is critical to examine the mechanical properties and shape recovery ability of SMPs conditioned at relevant

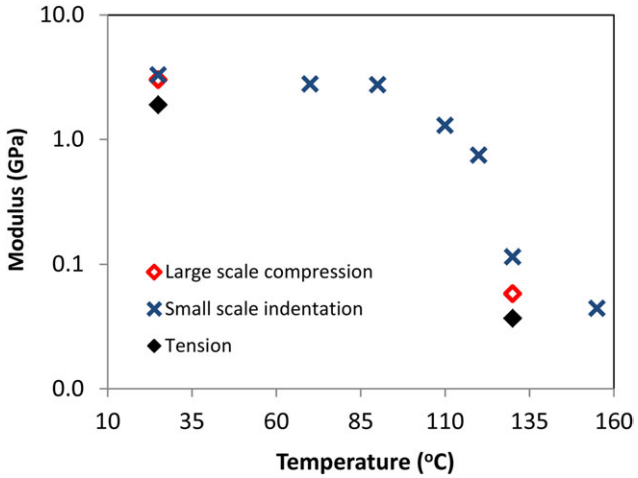

Figure 9. Temperature dependent modulus of the thermosetting SMP. [Color figure can be viewed in the online issue, which is available at wileyonlinelibrary.com.]

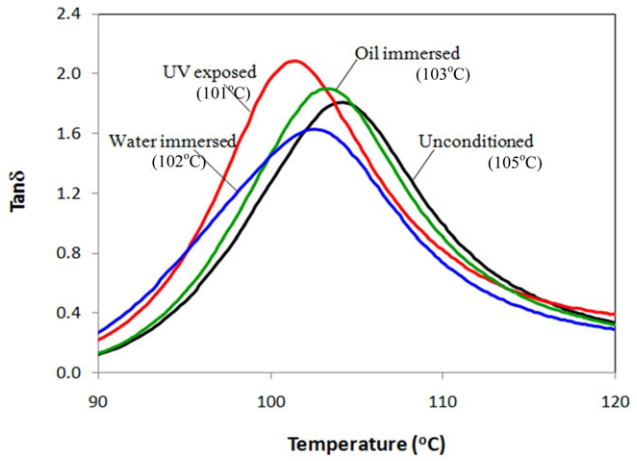

Figure 10. Tan(δ) curves of the original and conditioned SMPs measured using the DMA in torsion mode. Numbers shown in parentheses are the glass transition temperatures. [Color figure can be viewed in the online issue, which is available at wileyonlinelibrary.com.]

service environments so that the true reconfigurable ability of the SMPs can be predicted. Here the SMPs were conditioned in simulated service environments relevant to Air Force missions, including water immersion, lube oil immersion, and UV radiation. The glass transition temperatures of the conditioned SMPs were characterized with a dynamic mechanical analyzer (DMA), Model Q800 from TA Instrument. Tests were scanned from 25°C to 130°C with a heating rate of 2°C min^{-1}. The applied strain was 0.1% and the oscillating frequency was 10 Hz. Figure 10 depicts the Tan(δ) curves of the original and conditioned SMP specimens. From the curves, the glass transition temperature (T_g) of each SMP was determined [the peak of the Tan(δ) curve]. It is seen that the transition temperature of the original SMP occurs at –105°C. After conditioning, all SMPs are seen to exhibit a decrease in T_g in comparison to the unconditioned one. Among them, the UV exposed SMP has the largest decrease in T_g (101°C). The decrease in glass transition temperature in

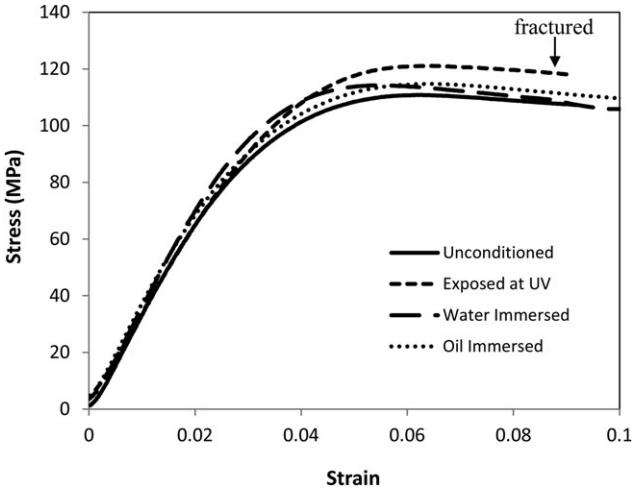

Figure 11. Stress–strain curves of the original and conditioned SMPs from large-scale compression tests (25°C).

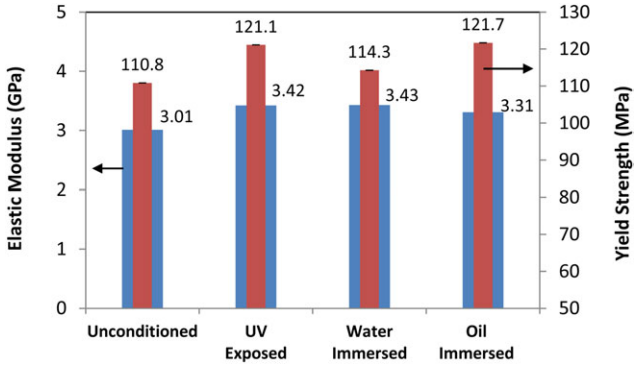

Figure 12. Elastic modulus and yield strength of the original and conditioned SMPs obtained from large-scale compression tests. [Color figure can be viewed in the online issue, which is available at wileyonlinelibrary.com.]

the SMP may be partially due to the presence of water content from various environmental conditionings (Recall that the standard UV exposure includes water sprays). The loosely bound water may have directly weakened the hydrogen bonding and therefore reduced the glass transition temperature.

The mechanical behaviors of the SMPs as results of environmental conditioning were examined using large-scale compression tests (maximum compression was limited to 10% strain). Figure 11 shows the stress–strain responses of the unconditioned and conditioned SMPs from the compressive tests at ambient temperature (glassy state). Under compressive loading, the SMP resins undergo significant plastic deformation following yielding. These observations are in contrast with the tensile testing results reported earlier, where the SMPs exhibited primarily linear elastic deformation and then fractured at a strain $<$ 5%.[12] Environmental conditionings have affected the microstructure and properties of the SMPs. The UV exposed SMP is seen to have limited ductility; the specimen became much brittle and broke into pieces before reaching the prescribed strain of 10%. Environmental conditionings have also increased the modulus and yield strength of the SMPs. Figure 12 shows the elastic moduli and yield strength of the unconditioned and

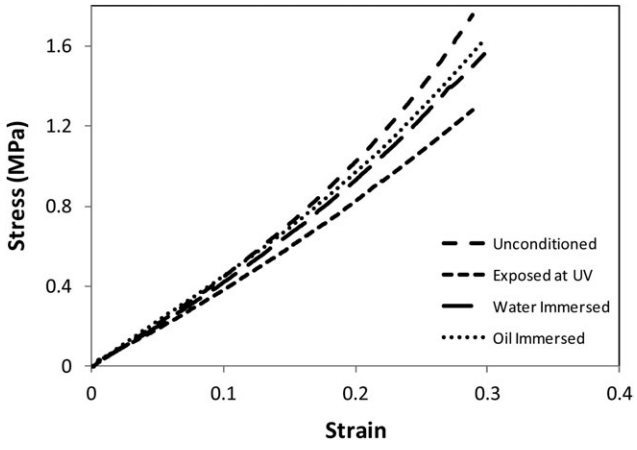

Figure 13. Stress–strain curves of the original and conditioned SMPs from large-scale compression tests (130°C).

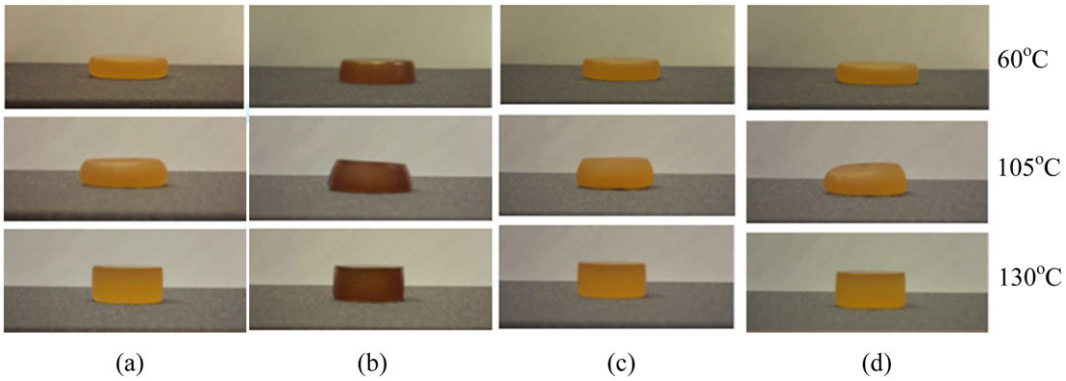

Figure 14. Pictures showing the recovery profiles of the original and conditioned SMPs under compressive loading. (a) Unconditioned, (b) UV exposed, (c) water immersed, and (d) oil immersed. [Color figure can be viewed in the online issue, which is available at wileyonlinelibrary.com.]

conditioned SMPs obtained from large-scale compression tests. All conditioned specimens are seen to exhibit higher modulus and yield strength than the unconditioned material, indicating the onset of brittleness when exposed to UV light and fluids. The oil and water conditioned samples are seen to have the greatest increases in modulus and yield strength, respectively.

Figure 13 shows the stress–strain responses of the original and conditioned SMPs from the compressive tests at 130°C (rubbery state). The maximum compression was limited to 30% strain. It is interesting to note that all conditioned SMPs become slightly softer as compared to the unconditioned one. All these findings are consistent with previous results obtained in tension.[12]

Shape Recovery Ability

The shape memory ability in polymers is driven by the amount of elastic strain generated during the deformation.[3–5] Deformation at low temperatures (glassy state) is difficult due to the high rigidity, therefore only small elastic strain can be generated in the material. On the other hand, deformation at elevated temperatures (rubbery state) is much easier due to the lower modulus, and a larger strain can be generated and stored in the material. To properly characterize the shape memory effect, the present SMP was activated in its rubbery state at a deformation temperature above its T_g: T_d=130°C. The large button shaped specimens from original and conditioned SMPs were deformed to a strain of 30% under compressive load and then "fixed" by cooling to room temperature while the deformation amount was kept constant. After cooling, the specimens were re-heated to selected temperatures (60°C, 75°C, 105°C, 115°C, 130°C). Figure 14 display the photographs of the shape recovery profiles of the SMPs corresponding to three temperatures: glassy temperature (60°C), transition temperature (105°C), and rubbery temperature (130°C). The shape recovery ability of each SMP is further quantified by the concept of linear shape recovery ratio, R.[12] For the compression experiments, R can be defined as follows

$$R = \left(1 - \frac{h_f}{h_i}\right) \cdot 100 \tag{7}$$

where h_i and h_f are the initial and final heights of the specimens corresponding to each recovery temperature. Each height represents an average of three measurements from the specimen. The shape recovery ratios of the SMPs at various temperatures are summarized in Table I. In all cases, the recoveries are negligible when the material is in the glassy state ($T_r < 75$°C) since the polymer chain segments are essentially frozen. During the broad band transition stage (105°C–115°C), partial recoveries are observed. The recovery in transition temperature range is not complete due to the coexistence of rigid, glassy segments and soft, rubbery segments. Complete or almost complete recoveries are seen to start to occur after 8 minutes of dwell time at elevated temperature (130°C). It is possible that the specimen might continue to recover, although at a much lower rate, with increase of dwell time at the elevated temperatures considered.

The environmental conditioning has clearly affected the mechanical and shape recovery properties of the SMPs. The UV exposed and water immersed SMPs are seen to have lesser recoveries compared to the unconditioned SMP and do not achieve the full recoveries in the end (Table I). Similar trends on shape recovery ratios have been reported using macroscopic tensile specimens[12] and nanoindentation,[15] albeit at different prescribed strain levels. It is also observed that the UV exposed SMPs exhibit much darker color than the other SMPs (see Figure 14). UV exposure is known

Table I. Tabulated Values for Linear Shape Recovery Ratios of the Original and Conditioned SMPs

Temperature (°C)	Unconditioned	UV conditioned	Oil conditioned	Water conditioned
60	0.00	0.00	0.00	0.00
105	57.14	34.08	57.60	55.68
115	85.04	72.39	89.08	79.04
130	101.28	93.78	100.86	94.76

to cause the photodegradation of polymers, including chain scission, oxidation, side-group destruction, etc.[30] which can potentially weaken the mechanical properties and shape recovery abilities of the polymers. Water immersion or spray allows the water diffuse into the polymer matrix, particularly the soft segments in the SMP. It has been reported that water absorbed in the SMP can weaken the hydrogen bonding between N—H and C=O groups.[31] Further, the water uptake in SMP can lead to an increase in the degree of phase separation or a decrease in the degree of phase mixing (frozen or hard phase and active or soft phase).[32] All these factors can deteriorate the mechanical responses of the polymers.

CONCLUSIONS

The thermomechanical behavior of a thermosetting SMP under compressive loading has been examined. The strain rate-dependent properties have been obtained under large-scale compression and small-scale indentation tests. In glassy state, the thermosetting SMP is observed to have much higher modulus and yield strength, and exhibit prolonged plasticity under compression than under tension. In rubbery state, the SMP behaves as a rubber-like material. When compressed, it has much higher modulus and has higher recovery forces. The overall temperature-dependent moduli of the SMP have been measured using high temperature indentation test. Results show that the SMP has a wider range of tunable stiffness under compression than under tension. Compression tests were further conducted to characterize the thermosetting SMP separately exposed to water, oil, and UV radiation. Results show that environmental conditioning affects the glass transition temperature, the mechanical properties, and the shape recovery abilities of the SMPs. It appears that all the conditioned SMPs exhibit a decrease in T_g as compared to the unconditioned one. The environmental conditionings also affect the modulus and yield strength of the SMPs: they increase the modulus in glassy state and decrease the modulus in rubbery state. The shape recovery ability of the SMP was assessed through compression tests. Results show that the materials have limited recoveries below the onset of glass transition temperature (T_g), partial recoveries during the transition region, and almost complete recoveries occur when the materials are in the rubbery state. The UV exposed and water-immersed SMPs exhibit lower shape recovery ratios as compared with the unconditioned one.

ACKNOWLEDGMENTS

This work was supported by the grants from NASA EPSCoR Research Infrastructure Development (RID) Program, Kentucky Space Grant Consortium (KSGC), and National Science Foundation (CMS-1130381).

REFERENCES

1. Lendlein, A.; Kelch, S. *Angew Chem. Int. Ed.* **2002**, *41*, 2034.
2. Beloshenko, V. A.; Varyukhin, V. N. ; Voznyak, Y. V. Russian Chem. *Rev.* **2005**, *74*(3), 265.
3. Liu, C.; Qin, H.; Mather, P. T. *J. Mater. Chem.* **2007**, *17*(16), 1543.
4. Xie, T. *Polymer*, **2011**, *52*, 4985.
5. Leng, J.; Lan, X.; Liu, Y.; Du, S. *Prog. Mater. Sci.* **2011**, *56*, 1077.
6. Ratna, D.; Karger-Kocsis, J. *J. Mater. Sci.* **2008**, *43*, 254.
7. Wei, Z. G.; Sandstrom, R.; Miyazaki, S. *J. Mater. Sci.* **1998**, *33*, 3743.
8. Gall, K.; Kreiner, P.; Turner, D.; Hilse, M. *J. Microelectromechan. Syst.* **2004**, *13*(3), 472.
9. Tobushi, H.; Hashimoto, T.; Ito, N.; Hayashi, S.; Yamada, E. *J. Intell. Mater. Syst. Struct.*, **1998**, *9*, 127.
10. Atli, B.; Gandhi, F.; Karst, G. *J. Intell. Mater. Syst. Struct.* **2009**, *20*(1), 87.
11. Liu, Y.; Gall, K.; Dunn, M. L.; Greenberg, A. R.; Diani, J. *Int. J. Plast.* **2006**, *22*, 279.
12. Tandon, G. P.; Goecke, K.; Cable, K.; Baur, J. *J. Intell. Mater. Syst. Struct.* **2009**, *20*, 2127.
13. McClung, A. J.; Tandon, G. P.; Baur, J. *Mech. Time-Depend. Mater.* **2012**, *16*, 205.
14. McClung, A. J.; Tandon, G. P.; Baur, J. *Mech. Time-Depend. Mater.* **2012**, DOI: 10.1007/s11043-011-9157-6. http: http://link.springer.com/article/10.1007/s11043-011-9157-6#
15. Lu, Y. C.; Fulcher, J. T.; Tandon, G. P.; Foster, D. C.; Baur, J. W. *Polym. Test.* **2011**, *30*, 563.
16. CRG Industries, LLC, Dayton, OH, 2009. http://crgindustries.com/product_data.htm.
17. Park, Y. J.; Pharr, G. M. *Thin Solid Films* **2004**, 447, 246.
18. Mesarovic, S. D.; Fleck, N. A. *Proc. R. Soc. Lond.* **1987**, *455*, 2707.
19. Lu, Y. C., Kurapati, S. N.; Yang, F. *J. Mater. Sci.* **2008**, *43*, 6331.
20. Ngan, A. H. W.; Tang, B. *J. Mater. Res.* **2004**, *17*(10), 2604.
21. Briscoe, B. J.; Fiori, L; Pelillo, E. *J. Phys., D: Appl. Phys.* **1998**, *31*, 2395.
22. Cheng, Y. T.; Cheng, C. M. *J. Mater. Res.* **2005**, *20*(4), 1046.
23. Lu, Y. C.; Jones, D. C.; Tandon, G. P.; Putthanarat, S.; Schoeppner, G. A. *Expert. Mechanic.* **2010**, *50*, 491.
24. Hertz, H. In Miscellaneous Papers; H, Hartz et al., Eds.; Macmillan: London, **1863**.
25. Oliver, W. C.; Pharr, G. M. *J. Mater. Res.* **1992**, *7*, 1564.
26. Oliver, W. C.; Pharr, G. M. *J. Mater. Res.* **2004**, *19*, 3.
27. Fujisawa, N.; Swain, M. V. *J. Mater. Res.* **2008**, *23*, 637.
28. Yeoh, O. H. *Rubber Chem. Technol.* **1993**, *66*, 754.
29. Charlton, D. J.; Yang, J.; The, K. K. *Rubber Chem. Technol.* **1994**, *67*, 481.
30. Rabek, J. F. Photodegradation of Polymers. Physical Characteristics and Applications; Springer Verlag: Berlin, **1996**.
31. Yang, B.; Huang, W. M.; Li, C.; Li, L. *Polymer* **2006**, *47*, 1348.
32. Pretsch, T., Jakob, I.; Muller, W. *Polym. Degrad. Stab.* **2009**, *94*, 61.